THE JOURNAL OF BIOLOGICAL CHEMISTRY VOL. 285, NO. 11, pp. 8155–8162, March 12, 2010

Microtubule-associated Protein-like Binding of the Kinesin-1 Tail to Microtubules*[S]

Received for publication, September 22, 2009, and in revised form, January 11, 2010 Published, JBC Papers in Press, January 12, 2010, DOI 10.1074/jbc.M109.068247

Mark A. Seeger and Sarah E. Rice[1]

From the Department of Cell and Molecular Biology, Northwestern University, Chicago, Illinois 60611

The kinesin-1 molecular motor contains an ATP-dependent microtubule-binding site in its N-terminal head domain and an ATP-independent microtubule-binding site in its C-terminal tail domain. Here we demonstrate that a kinesin-1 tail fragment associates with microtubules with submicromolar affinity. Binding is largely electrostatic in nature, and is facilitated by a region of basic amino acids in the tail and the acidic E-hook at the C terminus of tubulin. The tail binds to a site on tubulin that is independent of the head domain-binding site but overlaps with the binding site of the microtubule-associated protein Tau. Surprisingly, the kinesin tail domain stimulates microtubule assembly and stability in a manner similar to Tau. The biological function of this strong kinesin tail-microtubule interaction remains to be seen, but it is likely to play an important role in kinesin regulation due to the close proximity of the microtubule-binding region to the conserved regulatory and cargo-binding domains of the tail.

Kinesin-1 (KIF5b) is a molecular motor that transports cargo to the plus ends of microtubules. Kinesin-1 contains a homodimer of heavy chains, which are composed of N-terminal enzymatic heads, joined by a long coiled-coil to two C-terminal tails. *In vivo*, the C-terminal coiled-coil regions of the heavy chains are often, but not always, associated with the kinesin light chains, which help to mediate cargo binding. Kinesin-1-based transport is involved in a variety of cellular processes including the movement of intracellular vesicular cargoes and mitochondria, mRNA localization, and oocyte cytoplasmic streaming (1–4).

A plethora of *in vitro* biochemical investigations have elucidated many aspects of the walking mechanism of kinesin-1 (reviewed in Ref. 5), but only recently have studies begun to address the detailed structural mechanisms by which kinesin-1 is regulated and activated. Given the multitude of tasks kinesin-1 must accomplish in the cell, it is not surprising that there are many layers of regulation that enable kinesin-1 to transport distinct cargoes to specific locations throughout different types of cells (6, 7). The fundamental regulatory mechanism for kinesin-1 is the transition from a "folded" state to an "open" state. In the folded state the conserved "QIAK" sequence in the tail domain binds to the heads and inhibits their enzymatic activity by blocking the release of ADP. In the open state the heads are free to be activated by microtubules through the exchange ATP for ADP (8–10). Interestingly, a cryo-EM reconstruction of a head-tail-microtubule complex revealed that the tail could interact with both the head and the microtubule simultaneously (10). This result led to the idea that formation of this complex could enable kinesin-1 to "park," such that an enzymatically inactive motor remains tightly bound to the microtubule. Behavior of kinesin-1 molecules that is consistent with "parking" has been observed *in vitro* (11–13), but it is not known what purpose this may serve *in vivo*.

In vivo studies have demonstrated that the C-terminal tail of kinesin-1 contains an ATP-independent microtubule-binding site distinct from the head. Navone *et al.* (14) showed that both full-length kinesin-1 heavy chains and truncated kinesin-1 tails that were overexpressed in CV-1 cells decorated microtubules, and they surmised that kinesin-1 could actively slide one microtubule against another using its head- and tail-binding sites. Consistent with this, kinesin-1 has been shown to provide the force that drives the process of cytoplasmic streaming in *Drosophila* oocytes, where arrays of microtubules that are cross-linked by kinesin-1 churn to rapidly distribute yolk granules and other cytoplasmic components (4). This process requires the kinesin-1 heavy chain but not the light chain (3). Kinesin-1 was also shown to bundle microtubules in the fungus *Ustilago maydis*, and this activity was dependent on its C-terminal tail (15). In apparent contrast to the above results, both endogenous and expressed kinesin-1 have been shown to exhibit a diffuse cytoplasmic distribution with no obvious microtubule co-localization (16, 17). This discrepancy suggests that cell line-specific variations in the association or dissociation of kinesin-1 with its light chains or other tail-binding partners may alter the overall behavior of the motor *in vivo* by masking or revealing the tail microtubule-binding site.

Several factors have been identified that may act on the microtubule-binding site in the tail to affect microtubule cross-linking or cargo transport by kinesin-1. These include, but are not limited to, the kinesin-1 light chains,[2] the cargo adaptor protein milton (19), cytoplasmic dynein (20), and post-translational modifications of microtubules (21) or association of microtubule-associated proteins (MAP)[3] (22). The role of the tail-microtubule interaction has yet to be considered in the

* This work was supported, in whole or in part, by National Institutes of Health Grant GM072656 (to S. E. R.), Northwestern University Molecular Biophysics Training Program Grant 5T32 GM008382 (to M. A. S.), and the Northwestern University Malkin Scholarship Program (to M. A. S.).

[S] The on-line version of this article (available at http://www.jbc.org) contains supplemental Figs. S1–S5.

[1] To whom correspondence should be addressed: 303 E. Chicago Ave., Ward 8-321, Chicago, IL 60611. Tel.: 312-503-5390; Fax: 312-503-7912; E-mail: s-rice@northwestern.edu.

[2] Y. L. Wong and S. E. Rice, submitted for publication.

[3] The abbreviation used is: MAP, microtubule-associated protein.

model for kinesin-1 activity and regulation, and therefore the exact mechanism(s) through which the factors listed above affect the activity of the kinesin-1 holoenzyme *in vivo* is not clear. As a basic step in deciphering the contribution of the tail-microtubule interaction to the larger and seemingly complex process of kinesin-1 regulation, our work here identifies the location of the tail-microtubule-binding site, and shows that the kinesin-1 tail binds to microtubules with consequences very similar to MAP binding.

EXPERIMENTAL PROCEDURES

Constructs and Protein Purification—All proteins were grown in standard Luria-Bertani medium plus appropriate antibiotics in BL21(DE3) RP cells (Stratagene, La Jolla, CA). Dimeric human kinein-1 tail constructs contained residues 822–944. Single amino acid mutations were introduced using the QuikChange II kit (Promega, Madison, WI). Cysteines were introduced at residues Ala^{905} or Arg^{907}. For the Tail944 A905C Mutant A construct, alanines were substituted at residues Arg^{892}, Lys^{893}, Arg^{894}, Gln^{896}, and Gln^{897}. For the Tail944 A905C Mutant B construct, alanines were substituted at residues Arg^{901}, Lys^{903}, Arg^{907}, Lys^{909}, Asn^{910}, Arg^{913}, and Arg^{914}. For the Tail944 A905C Mutant A+B construct, the alanine mutations of both the Mutant A and Mutant B constructs were combined. The kinesin tail constructs contain a N-terminal histidine hexamer tag, which facilitated purification of the protein on Talon resin (Clontech, Mountain View, CA). Kinesin tail proteins were quantified by the Lowry protein assay (23), and all concentrations were reported as dimers. A synthetic tail peptide spanning residues 892–914, which contains the putative microtubule-binding site, was obtained from Bio-Synthesis Inc., Lewisville, TX. K349 G234A, a monomeric human kinesin-1 head construct spanning residues 1–349 and containing a G234A mutation in its Switch I domain, which allows it to bind to microtubules in its low affinity ADP-bound state (24), was purified as previously described (10), and quantified by Coomassie Protein Assay (Thermo Fisher Scientific, Rockford, IL). A full-length human Tau construct (hTau-40) containing a N-terminal histidine hexamer tag was purified and quantified the same as the kinesin tail constructs. Tubulin was purified from porcine brains as previously described (25), stored in aliquots at −80 °C, and clarified by centrifugation at 100,000 × *g* prior to use. Paclitaxel-stabilized microtubules were centrifuged through a 40% (v/v) glycerol cushion to remove any unpolymerized tubulin before use. The C-terminal 10–20 amino acids of α- and β-tubulin were removed by treatment with subtilisin (26).

Microtubule Co-sedimentation Assay—Tubulin was polymerized into microtubule filaments stabilized with paclitaxel, and quantified by absorbance measurements at 280 nm. Various concentrations of microtubules were mixed with constant concentrations of ligand in Binding Buffer (25 mM HEPES, pH 6.8, 2 mM $MgCl_2$, 1 mM EGTA, 0.02% Tween 20 (v/v)) plus 200 mM NaCl (or as otherwise indicated) and 20 μM paclitaxel. Samples were allowed to equilibrate at room temperature for 15 min, centrifuged at 50,000 × *g* for 15 min, and both the supernatant (S) and pellet (P) were precipitated with an excess of 100% acetone overnight at −80 °C. The samples were then recovered by centrifugation, resuspended in SDS sample buffer, and equal amounts of supernatant and pellet were run on 4–20% Tris-HCl gradient gels (Bio-Rad). Gels were examined under UV light if fluorescein-labeled tails were used, and then stained with Coomassie Blue. Quantification of the relative amounts of tail in supernatants and pellets was performed using ImageJ (developed by Wayne Rasband, National Institutes of Health, Bethesda, MD). The dissociation constants measured by microtubule co-sedimentation represent the average and propagated error from at least three separate experiments.

Fluorescence Anisotropy Assay—Tail944 A905C or R907C were covalently labeled with fluorescein 5-maleimide as per the manufacturer's instructions (Invitrogen), and unreacted dye was removed through multiple passes through Amicon Ultracel-10K centrifugal filter devices (Millipore, Billerica, MA) followed by dialysis against Binding Buffer. 0.01 μM Fluorescein-labeled tail was combined with various concentrations of microtubules in Binding Buffer, 50 μl of sample was loaded in duplicate into an opaque 384-well plate (Greiner Bio-One, Monroe, NC), and anisotropy measurements were made in a Safire II fluorescence microplate reader (Tecan US, San Jose, CA) with 10 reads per well and excitation/emission wavelengths of 470/520 nm. Anisotropy (r) was calculated from the following equation,

$$r = (I_{\text{parallel}}G - I_{\text{perpendicular}})/(I_{\text{parallel}}G + 2I_{\text{perpendicular}}) \quad \text{(Eq. 1)}$$

where I is the intensity of the polarized light emitted at 520 nm in the parallel or perpendicular orientation relative to the incident light, and G is a unitless correction factor for the Tecan instrument experimentally determined to be 1.1113. The anisotropy data were fit with the KaleidaGraph 3.6 graphing program (Synergy Software, Reading, PA) to the following equation,

$$r_{\text{measured}} - r_{\text{free}} = r_{\text{bound}}[MT]/(K_d + [MT]) \quad \text{(Eq. 2)}$$

where r_{measured} is the measured anisotropy, r_{free} is the anisotropy of the ligand alone, r_{bound} is the anisotropy at saturating concentrations of microtubules, K_d is the dissociation constant, and $[MT]$ is the concentration of microtubules. Dissociation constants were determined from anisotropy measurements made from at least three independent experiments.

Microtubule Assembly Assay—The change in solution turbidity was used to detect the assembly of tubulin into microtubule filaments. 10 μM tubulin was clarified by centrifugation at 100,000 × *g* and prepared in Binding Buffer in a 96-well UV-visible transparent plate (Corning Life Sciences, Lowell, MA) on ice. 1 mM GTP, or 1 mM GTP + 10 μM Tail944 A905C Mutant A+B, 10 μM Tail944, 20 μM Tail peptide, or 10 μM hTau-40 was added to the tubulin, and the absorbance at 350 nm and 37 °C was measured immediately (within 30 s) for a period of 15 min. Measurements were repeated eight times per condition and averaged. To determine the ratio of ligand to tubulin necessary to induce microtubule assembly, aliquots of samples prepared as described above, except with varying concentrations of ligand, were centrifuged at 50,000 × *g* at 20 °C for 15 min, and equal amounts of the recovered supernatants and

pellets were run on acrylamide gels and stained with Coomassie Blue.

Microtubule Stability Assay—A 50 μM solution of tubulin was prepared in Binding Buffer + 1 mM GTP, and incubated for 15 min at 37 °C. The tubulin was then diluted 10-fold into Binding Buffer, Binding Buffer + 5 μM Tail944 A905C Mutant A+B, 5 μM Tail944, 20 μM Tail peptide, or 5 μM hTau-40. The diluted samples were split into five aliquots and incubated for 30 min under one of the following conditions: room temperature, ice, 5 mM $CaCl_2$ at room temperature, 500 mM NaCl at room temperature, or a further 5-fold dilution in Binding Buffer at room temperature. The samples were then centrifuged at 50,000 × *g* at 20 °C (the samples incubated on ice were centrifuged at 4 °C) for 15 min, and equal amounts of the recovered supernatants and pellets were run on acrylamide gels and stained with Coomassie Blue.

Electron Microscopy—5 μM tubulin was incubated in Binding Buffer + 1 mM GTP with or without 5 μM Tail944 or 5 μM Tail944 A905C Mutant A+B or 5 μM hTau-40 for 15 min at room temperature. 10 μl of sample was then immediately spotted onto 300-mesh formvar/carbon-copper grids (Ted Pella Inc., Redding, CA), incubated for 2 min, stained, and fixed with 5 drops of 1% uranyl acetate (w/v), incubated for 2 min, thoroughly rinsed with distilled water, and air dried for 15 min. Samples were imaged with a Tecnai G^2 Spirit transmission electron microscope (FEI, Hillsboro, OR). Micrographs were quantified with ImageJ, and the lengths and widths of microtubules were reported as the average of 100 individual filaments and the periodicity of the tail-tubulin complexes was reported as the average of 100 separate intervals from a single filament.

Circular Dichroism—0.5 mg/ml of Tail944 or Tail944 A905C Mutant A+B was prepared in 5 mM Tris, pH 8.0, + 100 mM NaCl. Circular dichroism spectra were collected on a J-815 circular dichroism spectrophotometer (JASCO Inc., Easton, MD) in a cuvette with a 0.1-cm path length at 20 °C in the 199–240 nm wavelength range. Spectra were collected in triplicate from three separate samples and averaged after subtracting the spectrum of the buffer alone.

RESULTS

A Truncated Tail Construct Binds Tightly to Microtubules—A microtubule-binding site in the C-terminal tail domain of kinesin-1 has been identified both *in vitro* and in cells (9, 12, 14), but the affinity of this interaction has not been measured and its exact location has not been mapped. We created a dimeric tail construct consisting of residues 822–944, hereafter referred to as Tail944 (Fig. 1*A*). This construct contains approximately seven turns of the predicted coiled-coil structure, which enables the tail to dimerize. The microtubule-binding site is located at the boundary between the predicted coiled-coil and the globular C-terminal domain of the tail (12). Directly adjacent to the predicted microtubule-binding site is the conserved QIAK regulatory sequence that has been shown to inhibit the initial release of ADP from the kinesin motor domain (9, 11, 12). The extreme C-terminal 19 residues of the kinesin tail (residues 945–963) are susceptible over time to proteolytic cleavage when kinesin constructs are purified from bacteria. We found that a kinesin-1 tail construct containing an intact extreme

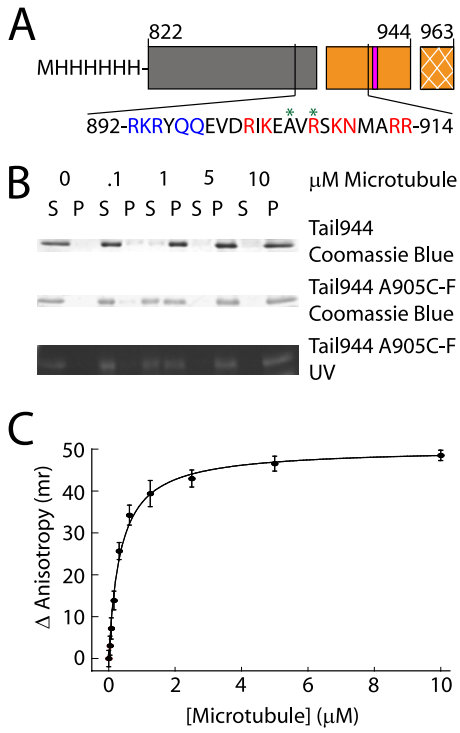

FIGURE 1. **A kinesin-1 tail construct binds to microtubules with a submicromolar affinity.** A schematic representation of the tail constructs used in this work is shown in *A*. The regions of the tail are indicated as follows: coiled-coil (*gray box*), microtubule-binding and regulatory domain (*orange box*), and the extreme 19 C-terminal residues not included in these tail constructs (*cross-hatched orange box*). Residues (919–922) are critical for regulation of enzymatic activity, and are indicated by a *pink bar*. The amino acid sequence of the putative microtubule-binding site in the tail is also shown. Residues mutated to alanine in Mutant A are highlighted in *blue*, residues mutated to alanine in Mutant B are highlighted in *red*, and sites where fluorescein was attached are indicated with a *green asterisk*. Gels used to measure the affinity of Tail944 or Tail944 R907C-fluorescein (*F*) for microtubules by co-sedimentation are shown in *B* (*S* = supernatant or unbound tail, *P* = pellet or bound tail). The Tail944 R907C-F gel was also examined under UV light to demonstrate the specificity of the fluorescein labeling. Fluorescence anisotropy data for determining the affinity of Tail944 R907C-F for microtubules is shown in *C*. K_d values from both assays are reported in Table 1. Fluorescence anisotropy data are reported as the mean ± S.E. for three experiments.

C-terminal region (residues 822–963) exhibited microtubule-binding behavior similar to the Tail944 construct (supplemental Fig. S1*A* and Table 1). Therefore, because residues 945–963 did not affect the tail-microtubule interaction, they were not included in the tail constructs used in subsequent experiments.

The affinity of the tail-microtubule interaction was measured using the two independent approaches of microtubule co-sedimentation and fluorescence anisotropy. We found that co-sedimentation was the more accurate approach for determining low-affinity interactions, and fluorescence anisotropy was more accurate for evaluating high-affinity interactions. Microtubule co-sedimentation assays using unlabeled Tail944 or fluorescein-labeled Tail944 revealed that the tail-microtubule affinity was not significantly affected by the labeling procedure (Fig. 1*B* and Table 1). Similar dissociation constants were measured by fluorescence anisotropy with the fluorescein probe attached at positions 905 or 907 of the tail (Table 1), indicating that the change in anisotropy is due to tail-microtubule binding and not a localized effect on the fluorescein probe. Both assays yielded complementary results in the 0–10 μM

TABLE 1

Summary of binding data showing that the kinesin-1 tail-microtubule interaction is electrostatic in nature, and is mediated by the basic residues in the 892–914 region of the tail and the acidic E-hooks of tubulin ($\alpha\beta$ = wild-type microtubules, $\alpha_s\beta_s$ = subtilisin-treated microtubules)

See Figs. 1, supplemental S1*A*, S2*B*, and S3 for microtubule co-sedimentation and fluorescence anisotropy experiments. All dissociation constants are reported as the mean ± S.E. for three experiments

Ligand	Microtubule	K_d	
		Microtubule co-sedimentation	Fluorescence anisotropy
		μM	
Tail944	$\alpha\beta$	0.45 ± 0.15	
Tail944 R907C-F	$\alpha\beta$	0.65 ± 0.21	0.46 ± 0.02
Tail963 R907C-F	$\alpha\beta$	0.56 ± 0.12	0.51 ± 0.07
Tail944 A905C-F	$\alpha\beta$	0.65 ± 0.14	0.35 ± 0.03
Tail944 A905C-F Mutant A	$\alpha\beta$	12.5 ± 2.2	ND[a]
Tail944 A905C-F Mutant B	$\alpha\beta$	3.8 ± 1.4	ND
Tail944 A905C-F Mutant A+B	$\alpha\beta$	16.7 ± 7.1	ND
Tail944 R907C-F	$\alpha_s\beta_s$	4.06 ± 2.9	3.17 ± 0.36

[a] ND, not determined.

microtubule range, but above 10 μM microtubules there was significant light scattering in the fluorescence anisotropy assay, therefore the microtubule co-sedimentation assay was used exclusively in situations were saturated binding occurred at microtubule concentrations greater than 10 μM (Fig. 1*C* and Table 1). Our results from both experiments demonstrated that the tail binds to microtubules with a very high affinity even under the relatively high ionic strength conditions used in our assays ($K_d \approx 0.5$ μM in 200 mM NaCl). We subsequently used the same microtubule co-sedimentation and fluorescence anisotropy assays to probe the details of the tail-microtubule interaction.

The Tail-Microtubule Interaction Is Electrostatic—The tail-microtubule interaction was strongly influenced by the ionic strength of the binding buffer, suggesting that binding was largely electrostatic. Fluorescence anisotropy measurements were made in the presence of 100–300 mM NaCl, and dissociation constants ranged from 0.09 ± 0.01 μM at 100 mM NaCl to a lower bound of >8.13 ± 1.76 μM at 300 mM NaCl (supplemental Fig. S1*B*). An intermediate dissociation constant of 0.46 ± 0.02 μM was measured at 200 mM NaCl, and all subsequent binding experiments in this work were performed in the presence of 200 mM NaCl and 25 mM HEPES, pH 6.8, unless otherwise indicated.

To further dissect the nature of the tail-microtubule interaction, several tail constructs were made in which the basic amino acids in the region of the tail at the boundary between the predicted coiled-coil and the conserved regulatory sequence were mutated to alanine (Fig. 1*A*). The ability of these constructs to bind microtubules was then assessed in microtubule co-sedimentation and fluorescence anisotropy assays. The microtubule co-sedimentation assays indicated that tail binding was not saturated in the presence of 10 μM microtubules for the Tail944 A905C-F (the A905C tail mutant labeled with fluorescine-5-maleimide, see "Experimental Procedures") Mutant A, Mutant B, or Mutant A+B constructs. Therefore the dissociation constants were determined exclusively from microtubule co-sedimentation data (Table 1 and supplemental Fig. S2*B*). The alanine substitutions in both the Mutant A and Mutant B constructs had significant effects on the K_d for microtubule binding. Mutant B had a 6-fold decrease in microtubule affinity, Mutant A had a 20-fold decrease, and Mutant A+B had a 25-fold decrease.

To test whether the difference in affinities observed for the Tail944 and Tail944 Mutant A+B constructs was due to a disruption in the secondary structure, the CD spectra of Tail944 and Tail944 Mutant A+B were compared. The spectra showed essentially identical α-helical content for both constructs (supplemental Fig. S2*A*), suggesting that the decrease in affinity was due to the removal of the positively charged tail residues in the mutant and not a disruption of the tail coiled-coil dimeric structure. Based on these results, we conclude that the microtubule-binding site in the tail extends from residue 892 to 914, containing the last few turns of the predicted coiled-coil and then continuing up to but not including the conserved QIAK regulatory region. This is compatible with previous results showing that kinesin-1 tail peptides containing either residues 889–918 or 904–933 were able to bind to microtubules (12). Our results suggest that the tail-microtubule association is mediated largely by complementary electrostatic interactions between the tail and microtubule.

The Putative Tail-binding Site Includes the Tubulin E-hooks—A cryo-EM reconstruction of Tail944 chemically cross-linked to the monomeric kinesin-1 head and then decorated on microtubules indicated that the tail made contact with the microtubule at the "h10-s9" loop between helix 10 and sheet 9 of both α- and β-tubulin (10). The h10-s9 loop contains several acidic residues, and is in close proximity to the C-terminal E-hook of tubulin, which is rich in glutamic acid residues, but is poorly ordered and therefore not visible in cryo-EM structures of microtubules (10). To test whether the E-hook of tubulin interacts with the tail, polymerized tubulin was treated with subtilisin, a serine protease that cleaves the C-terminal 10–20 amino acids from α- and β-tubulin. The subtilisin-treated microtubules were then used in microtubule co-sedimentation and fluorescence anisotropy assays as previously described (supplemental Fig. S3). The tail bound to subtilisin-treated microtubules with an ~6-fold greater dissociation constant relative to wild-type microtubules (see Table 1). Increased concentrations of subtilisin-treated microtubules could still bind all of the tail, indicating that the removal of the E-hooks inhibited but did not abolish tail binding. Therefore, the tail-binding site on tubulin includes the E-hooks and an additional site, such as the h10-s9 loop of α- and β-tubulin.

The Tail and Tau-binding Sites Overlap—MAPs such as Tau and MAP2 bind to helix 11, helix 12, and the E-hooks of α- and

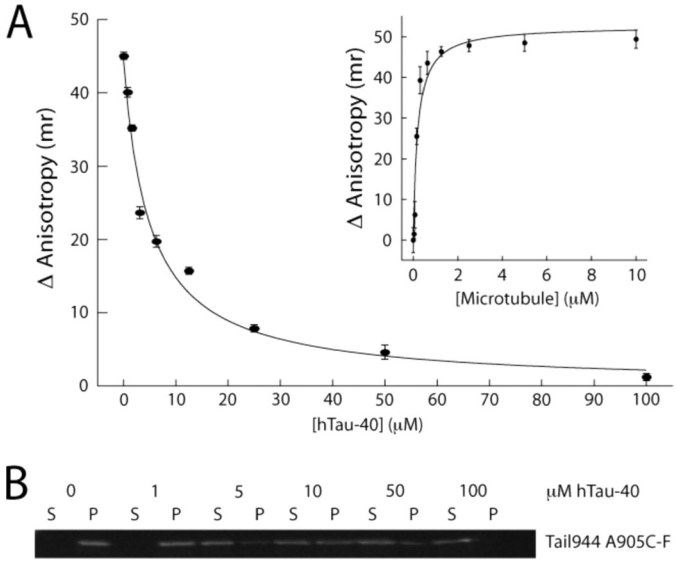

FIGURE 2. **The kinesin-1 tail and Tau compete for the same binding site on microtubules.** Tail944 A905C-F binds to microtubules with an affinity of 0.20 ± 0.052 μM in 100 mM NaCl (*A, inset*), as measured by fluorescence anisotropy. The binding of the same tail construct is inhibited in a concentration-dependent fashion by hTau-40 as measured by fluorescence anisotropy (*A*) and microtubule co-sedimentation (*B*, gel shows the amount of bound (*P*) and free (*S*) tail in the presence of increasing concentrations of Tau). The *solid line* in *A* is a fit to a simple competitive inhibition model (r^2 = 0.99), with half-maximal inhibition at 4.9 μM Tau. Fluorescence anisotropy data are reported as the mean ± S.E. for three experiments.

β-tubulin (27). Given the observed inhibitory effect of subtilisin treatment on kinesin-1 tail binding, it seemed likely that the tail and microtubule-associated proteins, such as Tau, would have similar or overlapping binding sites on tubulin. Therefore, we tested whether Tau competes with the tail for the same microtubule-binding site. The hTau-40 construct used in our studies contains four microtubule-binding sites, and binds to microtubules with a dissociation constant of 1–5 μM, as estimated by a microtubule co-sedimentation assay (supplemental Fig. S4). Because hTau-40 binds relatively weakly to microtubules at 200 mM NaCl, experiments were performed in the presence of a reduced salt concentration (100 mM NaCl, 25 mM HEPES, pH 6.8). Under these buffer conditions, Tail944 R907C-F bound to microtubules with a dissociation constant of 0.20 ± 0.05 μM measured by fluorescence anisotropy (Fig. 2, *inset*), and tail binding was clearly saturated at 5 μM microtubules. The anisotropy of 0.01 μM Tail944 in the presence of 5 μM microtubules and increasing concentrations of hTau-40 was measured (Fig. 2). Roughly 50 μM hTau-40 was required to completely inhibit tail binding to microtubules, and half-maximal inhibition of tail binding was observed at 4.9 μM hTau-40, which is close to the K_d of hTau-40 binding to microtubules under these conditions (supplemental Fig. S4). Thus, hTau-40 was able to competitively inhibit the tail-microtubule interaction, indicating that the kinesin-1 tail and hTau-40 compete for the same binding site on tubulin. These results further suggest that the helix 11 and helix 12 of tubulin, in addition to the h10-s9 loop and the E-hook, may be involved in tail binding.

In the cryo-EM reconstruction of the kinesin-1 head-tail-microtubule complex, the tail appears to simultaneously contact both the head and the microtubule. Both tails and heads bind strongly to microtubules under the conditions used to produce this structure, and this study did not determine whether tails and heads compete to some extent for the same binding site on the microtubule (10). Given the fact that the tail and Tau appear to bind to similar regions of tubulin, and that it has been observed that the kinesin-1 head binds to a site on tubulin distinct from both the Tau-binding site (reviewed in Ref. 29) and the tail-binding site (10), it seemed likely that the kinesin-1 head and tail would bind independently to microtubules. To test this hypothesis, two microtubule co-sedimentation experiments were designed. In the first experiment 1 μM Tail944 was bound to 2.5 μM microtubules in the presence of saturating concentrations of the monomeric kinesin-1 head construct K349 G234A, which binds tightly to microtubules regardless of nucleotide state (10). In the second experiment 1 μM K349 G234A was bound to 2.5 μM microtubules in the presence of saturating concentrations of Tail944. The results of these experiments showed that saturating concentrations of head did not inhibit or facilitate tail binding, and that saturating concentrations of tail did not inhibit or facilitate head binding (supplemental Fig. S5). Therefore, the tail-binding site on tubulin is completely distinct from the head-binding site, but overlaps significantly with the hTau-40-binding site.

The Tail Stimulates Microtubule Assembly and Stability—MAPs, such a Tau, are known to stimulate the assembly of microtubule filaments. Because Tau and the kinesin-1 tail appear to bind in the same vicinity on tubulin, we wished to test whether the tail may have an effect on microtubule assembly and stability similar to Tau. Microtubule assembly was monitored by observing the change in turbidity of a solution of unpolymerized tubulin in the presence of GTP and additional ligands. hTau-40, Tail944, or a peptide containing residues 892–914 of the microtubule-binding site of the kinesin-1 tail, in the presence of tubulin and GTP, produced a significant increase in turbidity (absorbance at 350 nm) relative to tubulin alone + GTP after 15 min at 37 °C (Fig. 3*B*). Tubulin + Tail944 A905C Mutant A+B did not affect the absorbance, demonstrating that the change in solution turbidity depends on the ability of the added ligand to bind to tubulin. The tail and tail peptide appeared to stimulate the polymerization of tubulin significantly faster than hTau-40 because the absorbance readings of tubulin in the presence of the tail or tail peptide samples reached their maximum values ~5–15 min faster than the absorbance readings of the hTau-40 samples. Addition of 500 mM NaCl to the microtubules polymerized in the presence of ligand caused a decrease in the absorbance back down to the baseline reading defined by tubulin alone (data not shown), showing that the observed increase in turbidity due to ligand-induced tubulin polymerization was reversible. Lower concentrations of ligand were unable to stimulate this rapid change in absorbance (data not shown), suggesting that at least a 1:1 ratio between tubulin and tail or hTau-40 was necessary to induce the complete polymerization of microtubule filaments under these reaction conditions. To determine the exact molar ratio between kinesin tail and tubulin required for polymerization, tubulin was incubated with GTP and various concentrations of Tail944, Tail944 A905C Mutant A+B, tail peptide, or hTau-40. A microtubule co-sedimentation assay was then performed.

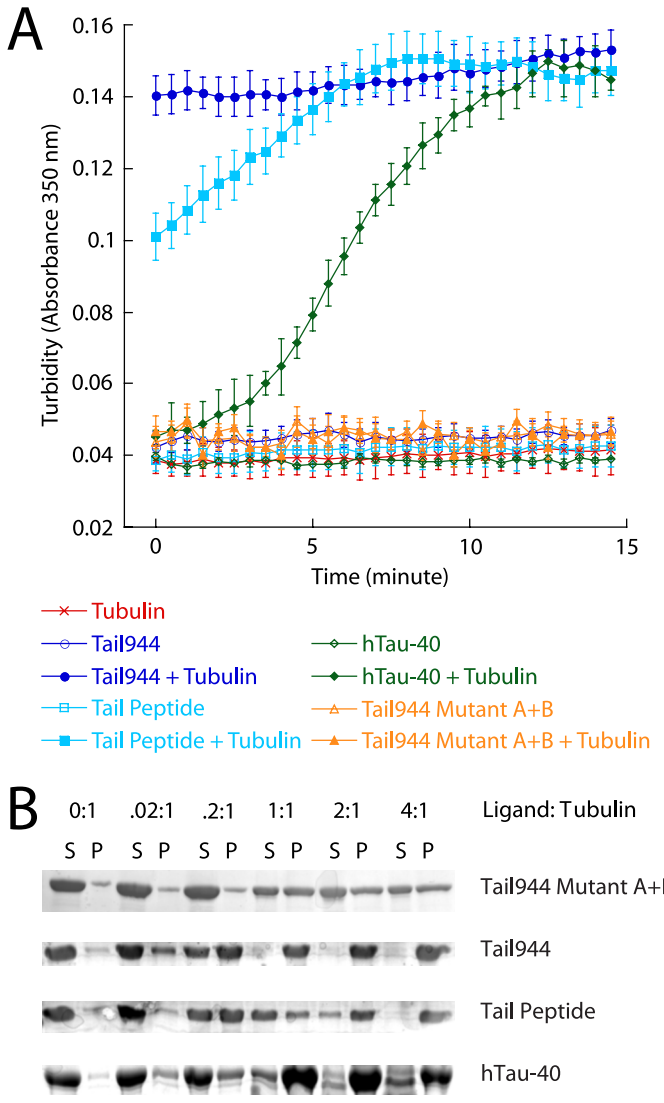

FIGURE 3. **The kinesin-1 tail stimulates microtubule assembly in a manner similar to Tau.** The change in solution turbidity of tubulin alone or tubulin plus fixed concentrations of ligand (Tail944, Tail944 A905C Mutant A+B, Tail Peptide, or hTau-40) was monitored over 15 min in *A*. Turbidity data are reported as the mean ± S.E. for eight experiments. Tubulin was mixed with increasing concentrations of ligand (Tail944, Tail944 A905C Mutant A+B, Tail Peptide, or hTau-40), and the amount of assembled tubulin (*P*) *versus* disassembled tubulin (*S*) was compared by gel electrophoresis in *B*.

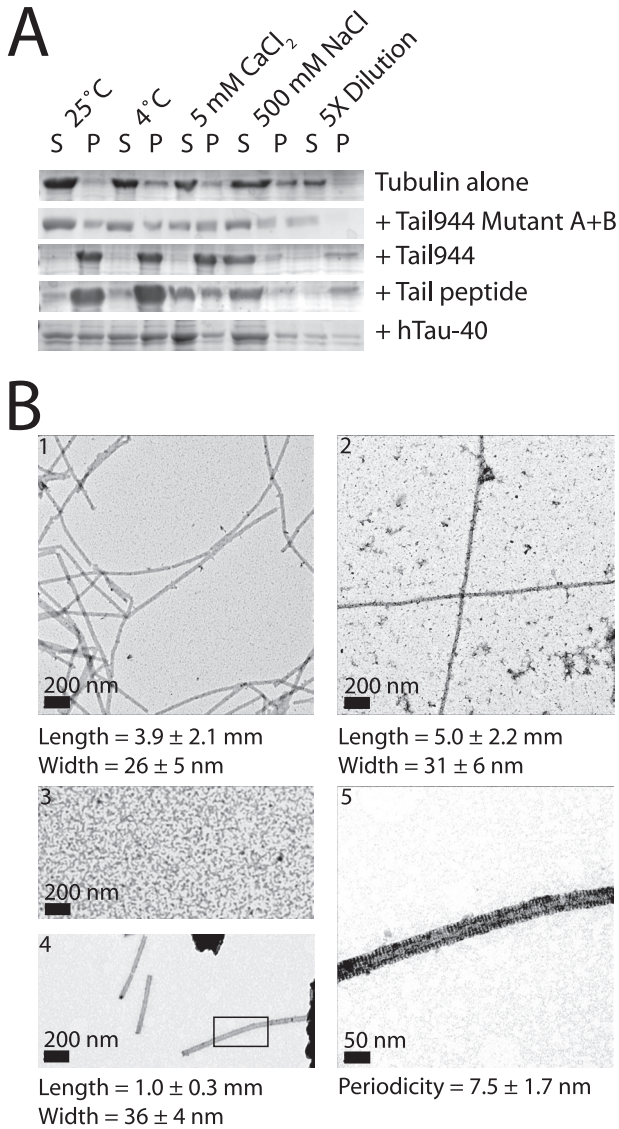

FIGURE 4. **The kinesin-1 tail stimulates microtubule stability in a manner similar to Tau.** Tubulin with or without ligand (Tail944, Tail944 A905C Mutant A+B, Tail Peptide, or hTau-40) was incubated under various microtubule-destabilizing conditions (shift to 4 °C, $CaCl_2$, NaCl, or dilution), and the amount of assembled microtubules (*P*) *versus* disassembled tubulin (*S*) was compared by gel electrophoresis in *A*. Representative negative stain electron micrographs of paclitaxel-stabilized microtubules (*panel 1*) or tubulin polymerized without paclitaxel in the presence of hTau-40 (*panel 2*), Tail944 A905C Mutant A+B (*panel 3*), or Tail944 (*panels 4* and *5*) are shown in *B*. The *boxed area* in *panel 4* is magnified in *panel 5* to show the 8-nm periodic pattern of density along the edges of the microtubule. Length, width, and periodicity values are reported as the mean ± S.D. of 100 measurements.

Tubulin was completely assembled into microtubule filaments in the presence of equal molar amounts of Tail944 or hTau-40 or a 4:1 molar ratio of tail peptide to tubulin, but Tail944 A905C Mutant A+B was unable to stimulate complete assembly at any concentration tested (Fig. 3*A*). These results indicate that, like Tau, the kinesin tail can stimulate microtubule polymerization, and that this function is localized to its microtubule-binding domain.

Tau is also known to stabilize microtubule filaments against various conditions that would cause naked microtubules to depolymerize. To test if the kinesin-1 tail had a similar effect on microtubule stability, polymerized tubulin in the presence of Tail944, Tail944 A905C Mutant A+B, tail peptide, or hTau-40 was incubated for 30 min at room temperature, on ice, in the presence of 5 mM $CaCl_2$, in the presence of 500 mM NaCl, or diluted below the microtubule critical concentration. A microtubule co-sedimentation assay was then performed. Tail944 A905C Mutant A+B was unable to completely stabilize microtubules under any of the conditions tested. Tail944, tail peptide, and hTau-40 all were able to stabilize microtubules against incubation at room temperature, incubation on ice, and dilution below the microtubule critical concentration (Fig. 4*A*). None of the ligands were able to stabilize microtubules in the presence of 500 mM NaCl, which was most likely due to an inability of the ligands to bind to tubulin under high salt conditions (supplemental Figs. S1*B* and S4). Interestingly, only the Tail944 construct was able to robustly stabilize microtubules in the presence of 5 mM $CaCl_2$. These results suggest that the

kinesin-1 tail, specifically residues 892–914, has a MAP-like ability to promote microtubule assembly and stability.

To confirm that the tubulin structures produced in the assembly and stability assays were in fact ordered microtubule filaments, tubulin was polymerized in the presence of paclitaxel or alternatively, in the absence of paclitaxel with Tail944, Tail944 A905C Mutant A+B, or hTau-40, and examined by electron microscopy. Tail944 A905C Mutant A+B did not stimulate the formation of any sort of ordered structure. Paclitaxel caused tubulin to polymerize into long flexible microtubule filaments with a width of ~26 ± 5 nm, which is what would be expected for a 13-protofilament microtubule. hTau-40 caused tubulin to polymerize into long straight microtubule filaments with a width of ~31 ± 6 nm. Last, Tail944 caused tubulin to polymerize into relatively straight but shorter (1 μm on average) microtubule filaments with a width of 36 ± 4 nm. Strikingly, at high magnification the Tail944-stabilized microtubules appeared to have an 8-nm periodicity (7.5 ± 1.7 nm) along their edges, which may be attributed to the bound tail protein (Fig. 4*B*). This suggests that the tail does in fact bind to a specific site on the microtubule. The origin of the observed 8 nm periodicity would have to be corroborated by higher resolution methods, but it is interesting to note that an 8-nm interval corresponds to one tail dimer bound per α-β-tubulin heterodimer, the minimal stoichiometry that was demonstrated to be required for tail-induced microtubule assembly and stability (Figs. 3*B* and 4*A*). These images show that the kinesin-1 tail is able to stimulate the assembly and stability of ordered microtubule filaments in a manner that is similar but not identical to Tau or paclitaxel.

DISCUSSION

We have shown that the kinesin-1 tail binds to microtubules with a submicromolar affinity in an electrostatic-dependent manner. The tail-microtubule binding affinity was measured with microtubule co-sedimentation and fluorescence anisotropy assays. K_d values determined by co-sedimentation are more accurate for the lower affinity interactions (1 μM $< K_d <$ 10 μM), because fluorescence anisotropy measurements are hampered by prohibitive amounts of light scattering at microtubule concentrations above 10 μM. On the other hand, for high-affinity interactions (0 μM $< K_d <$ 1 μM), fluorescence anisotropy was more accurate. The co-sedimentation assay was limited by the amount of protein that could be visualized and quantified on a gel. This necessitated the use of 0.1 μM tail, which is 10-fold higher than the concentration used in the fluorescence anisotropy assay. As a result, co-sedimentation assays used to measure high-affinity tail-microtubule interactions are likely to err toward an overestimate of K_d relative to the results obtained for the same constructs by fluorescence anisotropy. Despite these technical considerations, overall the two assays produced very complementary results (see Table 1).

Our subtilisin cleavage studies have shown that the tail binds to microtubules at a site that includes the tubulin E-hooks, and our competition binding experiments using kinesin tails and hTau-40 indicate that tails and MAPs bind to overlapping sites on tubulin. Similar to MAPs, the tail is also able to stimulate assembly and promote stability of microtubules. A comparison of tail- and Tau-stabilized microtubules reveals similarities and differences between these interactions. Both the tail and Tau bind longitudinally along the outer edge of the microtubule protofilament in cryo-EM reconstructions (10, 27). hTau-40 has four microtubule-binding sites arranged in tandem, and because the kinesin-1 tail is a dimer, it has two adjacent microtubule-binding sites (one on each heavy chain). These sites could potentially form two lateral contacts that bridge two protofilaments, in contrast to the four longitudinal contacts along a single protofilament as observed for Tau. This potential binding mode could explain several of our observations. 1) Unlike Tau, the tail does not interfere with kinesin-1 head binding because it does not span the α-β-tubulin interface, where heads have been shown to bind (28, 29). 2) Fig. 4*B* electron micrographs show that hTau-40 stimulates the formation of long microtubule filaments because it stabilizes microtubules in the longitudinal direction, whereas the tail stimulates the formation of shorter segments of microtubule filaments because it stabilizes microtubules in the lateral direction. 3) The tail stimulates microtubule assembly at a rate that is significantly faster than hTau-40 (Fig. 3*A*) because the tail induces the formation of many short microtubule filaments from many nucleation sites, whereas hTau-40 induces the formation of fewer but longer microtubule filaments from fewer nucleation sites. 4) Stimulation of microtubule assembly and stability by the Tail peptide is not nearly as robust as the Tail944 construct because the Tail peptide is a monomer and therefore cannot bridge adjacent protofilaments. Taken together, these results suggest that the kinesin-1 tail and hTau-40 act at the same site on tubulin to stimulate polymerization, and the specific structure of the microtubule filament produced depends on the adjacent *versus* tandem arrangement of the individual microtubule-binding sites in the tail and hTau-40, respectively.

Microtubules are a binding hub for many proteins in the cell, and a large subset of these proteins, including Tau, MAP1b, and MAP2, interact with the C terminus of tubulin (reviewed in Ref. 30). The tail domain of another kinesin family member, Ncd, has been shown to bind microtubules with a submicromolar affinity in the vicinity of the tubulin C terminus, and promote microtubule assembly and stability (31–33). Similarly, binding of a poly-L-lysine peptide to tubulin or cleavage of the tubulin C terminus by subtilisin both induce tubulin to spontaneously assemble into microtubules (34, 35). Therefore, masking the acidic charges of the tubulin E-hooks via ligand binding seems to promote microtubule filament formation and stability.

This study has revealed the location, strength, and *in vitro* consequences of a potentially important interaction between the kinesin tail domain and the microtubule lattice that may regulate motor and/or microtubule function. It remains to be seen what biological functions could be served by a strong tail-microtubule interaction that stabilizes the microtubule filament, but several lines of investigation suggest that this interaction may in fact be biologically relevant. Kinesin-1 exists as a dimer, and only one tail is required to inhibit the ATPase activity of both heads (18). Therefore, a variety of scenarios for kinesin-1 activity and regulation that involve the tail microtubule-binding site are possible. For example, kinesin-1 in its compact inactive state or with cargo or the motor domains bound to one

of its tails could diffuse along or tether to microtubules via its free tail, or perhaps a free tail in close proximity to the microtubule could enhance the processivity of kinesin-1-based transport by keeping the molecule in close contact with the microtubule if the motor domains were to dissociate (a process that we would argue has already been observed by Friedman and Vale (13)). Kinesin-1 has also been shown to cross-bridge, slide, and buckle microtubules *in vivo* (15), processes that necessitate stable microtubule filaments and strong microtubule-binding sites in both the head and tail domains.

Given the multitude of tasks kinesin-1 must accomplish, it is not unexpected that there would be a variety of ways in which the head and tail domains are regulated or interact with their microtubule substrate. It is also not surprising that there are seemingly contradictory experimental results concerning the role of the tail-microtubule interaction in "normal" kinesin-1 activity, because these experiments are likely revealing different specific mechanisms that kinesin-1 utilizes to regulate and accomplish different tasks in the cell. Further experimentation will be necessary to reveal the *in vivo* purpose of the MAP-like properties of the kinesin-1 tail.

Acknowledgments—We thank Dr. Lester Binder for the hTau-40 construct, Lennell Reynolds Jr., Northwestern University Cell Imaging Facility, for assistance with the electron microscopy, Dr. Arabela Grigorescu, Northwestern University Keck Biophysics Facility, for assistance with the circular dichrosim, Dr. Douglas Freymann for use of the fluorescence microplate reader, Park Packing Company for providing materials for tubulin purification, and members of the Rice laboratory for thoughtful suggestions and criticism.

REFERENCES

1. Sakamoto, R., Byrd, D. T., Brown, H. M., Hisamoto, N., Matsumoto, K., and Jin, Y. (2005) *Mol. Biol. Cell* **16,** 483–496
2. Cai, Q., Gerwin, C., and Sheng, Z. H. (2005) *J. Cell Biol.* **170,** 959–969
3. Serbus, L. R., Cha, B. J., Theurkauf, W. E., and Saxton, W. M. (2005) *Development* **132,** 3743–3752
4. Palacios, I. M., and St. Johnston, D. (2002) *Development* **129,** 5473–5485
5. Gennerich, A., and Vale, R. D. (2009) *Curr. Opin. Cell Biol.* **21,** 59–67
6. Hammond, J. W., Griffin, K., Jih, G. T., Stuckey, J., and Verhey, K. J. (2008) *Traffic* **9,** 725–741
7. Jacobson, C., Schnapp, B., and Banker, G. A. (2006) *Neuron* **49,** 797–804
8. Stock, M. F., Guerrero, J., Cobb, B., Eggers, C. T., Huang, T. G., Li, X., and Hackney, D. D. (1999) *J. Biol. Chem.* **274,** 14617–14623
9. Hackney, D. D., and Stock, M. F. (2000) *Nat. Cell Biol.* **2,** 257–260
10. Dietrich, K. A., Sindelar, C. V., Brewer, P. D., Downing, K. H., Cremo, C. R., and Rice, S. E. (2008) *Proc. Natl. Acad. Sci. U.S.A.* **105,** 8938–8943
11. Coy, D. L., Hancock, W. O., Wagenbach, M., and Howard, J. (1999) *Nat. Cell Biol.* **1,** 288–292
12. Yonekura, H., Nomura, A., Ozawa, H., Tatsu, Y., Yumoto, N., and Uyeda, T. Q. (2006) *Biochem. Biophys. Res. Commun.* **343,** 420–427
13. Friedman, D. S., and Vale, R. D. (1999) *Nat. Cell Biol.* **1,** 293–297
14. Navone, F., Niclas, J., Hom-Booher, N., Sparks, L., Bernstein, H. D., McCaffrey, G., and Vale, R. D. (1992) *J. Cell Biol.* **117,** 1263–1275
15. Straube, A., Hause, G., Fink, G., and Steinberg, G. (2006) *Mol. Biol. Cell* **17,** 907–916
16. Hollenbeck, P. J. (1989) *J. Cell Biol.* **108,** 2335–2342
17. Cai, D., Verhey, K. J., and Meyhöfer, E. (2007) *Biophys. J.* **92,** 4137–4144
18. Hackney, D. D., Baek, N., and Snyder, A. C. (2009) *Biochemistry* **48,** 3448–3456
19. Glater, E. E., Megeath, L. J., Stowers, R. S., and Schwarz, T. L. (2006) *J. Cell Biol.* **173,** 545–557
20. Ligon, L. A., Tokito, M., Finklestein, J. M., Grossman, F. E., and Holzbaur, E. L. (2004) *J. Biol. Chem.* **279,** 19201–19208
21. Reed, N. A., Cai, D., Blasius, T. L., Jih, G. T., Meyhofer, E., Gaertig, J., and Verhey, K. J. (2006) *Curr. Biol.* **16,** 2166–2172
22. Dixit, R., Ross, J. L., Goldman, Y. E., and Holzbaur, E. L. (2008) *Science* **319,** 1086–1089
23. Lowry, O. H., Rosebrough, N. J., Farr, A. L., and Randall, R. J. (1951) *J. Biol. Chem.* **193,** 265–275
24. Rice, S., Lin, A. W., Safer, D., Hart, C. L., Naber, N., Carragher, B. O., Cain, S. M., Pechatnikova, E., Wilson-Kubalek, E. M., Whittaker, M., Pate, E., Cooke, R., Taylor, E. W., Milligan, R. A., and Vale, R. D. (1999) *Nature* **402,** 778–784
25. Williams, R. C., Jr., and Lee, J. C. (1982) *Methods Enzymol.* **85,** 376–385
26. Rodionov, V. I., Gyoeva, F. K., Kashina, A. S., Kuznetsov, S. A., and Gelfand, V. I. (1990) *J. Biol. Chem.* **265,** 5702–5707
27. Al-Bassam, J., Ozer, R. S., Safer, D., Halpain, S., and Milligan, R. A. (2002) *J. Cell Biol.* **157,** 1187–1196
28. Seitz, A., Kojima, H., Oiwa, K., Mandelkow, E. M., Song, Y. H., and Mandelkow, E. (2002) *EMBO J.* **21,** 4896–4905
29. Marx, A., Müller, J., Mandelkow, E. M., Hoenger, A., and Mandelkow, E. (2006) *J. Muscle Res. Cell Motil.* **27,** 125–137
30. Maccioni, R. B., and Cambiazo, V. (1995) *Physiol. Rev.* **75,** 835–864
31. Karabay, A., and Walker, R. A. (1999) *Biochemistry* **38,** 1838–1849
32. Karabay, A., and Walker, R. A. (2003) *Biochem. Biophys. Res. Commun.* **305,** 523–528
33. Karabay, A., and Walker, R. A. (1999) *Biochem. Biophys. Res. Commun.* **258,** 39–43
34. Serrano, L., de la Torre, J., Maccioni, R. B., and Avila, J. (1984) *Proc. Natl. Acad. Sci. U.S.A.* **81,** 5989–5993
35. Lee, J. C., Tweedy, N., and Timasheff, S. N. (1978) *Biochemistry* **17,** 2783–2790